Neuroscience 153 (2008) 1190–1201

A NOVEL TRANSVERSE EXPRESSION DOMAIN IN THE MOUSE CEREBELLUM REVEALED BY A NEUROFILAMENT-ASSOCIATED ANTIGEN

H. MARZBAN, C.-T. KIM,[1] D. DOORN, S.-H. CHUNG AND R. HAWKES*

Department of Cell Biology and Anatomy, Hotchkiss Brain Institute, and Genes and Development Research Group, Faculty of Medicine, University of Calgary, 3330 Hospital Drive Northwest, Calgary, Alberta, Canada T2N 4N1

Abstract—The mammalian cerebellum is composed of a highly reproducible array of transverse zones, each of which is subdivided into parasagittal stripes. By using a combination of Purkinje cell antigenic markers and afferent tracing, four transverse zones have been identified: the anterior zone (AZ: ~lobules I–V), the central zone (CZ: ~lobules VI–VII), the posterior zone (PZ: ~lobules VIII-dorsal IX) and the nodular zone (NZ: ~ventral lobule IX+lobule X). Neurofilament-associated antigen (NAA) is an epitope recognized by a monoclonal antibody, which is expressed strongly in association with neurofilaments. During perinatal cerebellar development, anti-NAA immunocytochemistry reveals novel features of cerebellar organization. In particular, the CZ is reproducibly subdivided into anterior and posterior components. Between embryonic day 17 and postnatal day 7 NAA immunoreactivity is expressed selectively by a parallel fiber bundle that is restricted to lobule VII, thereby distinguishing the CZ anterior (lobules VIa, b) from the CZ posterior (lobule VII). The novel restriction boundary at lobule VII/VIII, which is also reflected in the morphology of the external granular layer and aligns with a gap in the developing Purkinje cell layer, precedes the morphological appearance of the posterior superior fissure between lobules VIb and VII. In addition, afferent axons to the CZ terminate in an array of parasagittal stripes that is probably a specific climbing fiber projection. Thus, the transverse zone architecture of the mouse cerebellum is more complex than had previously been appreciated.

Key words: stripes, zones, zebrin II, parallel fiber, climbing fiber, Purkinje cell.

The complex topography of the cerebellar cortex can be revealed by the expression patterns of numerous molecules. The primary organizer seems to be the Purkinje cell. In the adult, Purkinje cell expression patterns reveal a complex topography that is both highly reproducible (e.g. Brochu et al., 1990) and conserved across species (Sillitoe et al., 2005). The mouse cerebellum comprises four transverse zones: the anterior zone (AZ: ~lobules I–V), the central zone (CZ: ~lobules VI–VII), the posterior zone (PZ: ~lobules VIII–dorsal IX) and the nodular zone (NZ: ~ventral lobule IX+lobule X) (e.g. Ozol et al., 1999; Armstrong et al., 2000; Sillitoe and Hawkes, 2002). The transverse zones of the vermis are mirrored in the hemispheres. Each transverse zone is subdivided into a reproducible array of parasagittal stripes (e.g. revealed by using zebrin II/aldolase C expression in the AZ and PZ; Brochu et al., 1990; Eisenman and Hawkes, 1993; Ozol et al., 1999; Sillitoe and Hawkes, 2002; by using expression of the small heat shock protein HSP25 in the CZ and NZ; Armstrong et al., 2000). In addition to the compartmentation of the Purkinje cells, similar zone and stripe restrictions are seen in the expression patterns of granule cell markers (e.g. nitric oxide synthase; Hawkes and Turner, 1994: reviewed in Ozol and Hawkes, 1997). Finally, the zone and stripes topography is also reflected in the terminal fields of both mossy fibers (e.g. Gravel and Hawkes, 1990; Akintunde and Eisenman, 1994; Ji and Hawkes, 1994) and climbing fibers (e.g. Gravel et al., 1987; Wassef et al., 1992; Voogd et al., 2003; Apps and Garwicz, 2005; Sugihara and Quy, 2007 etc.), and in associated receptive field maps (Chockkan and Hawkes, 1994; Hallem et al., 1999; Gao et al., 2006 etc.). Cerebellar topography can be traced prenatally, and is apparently stable throughout development (e.g. Luckner et al., 2001; Marzban et al., 2007: reviewed in Herrup and Kuemerle, 1997; Armstrong and Hawkes, 2000; Larouche and Hawkes, 2006 etc.).

Monoclonal antibody 3A10 recognizes a peptide epitope—neurofilament-associated antigen (NAA)—that is co-expressed with neurofilaments in the adult brain (e.g. Serafini et al., 1996). The specific epitope(s) is unknown. In this report NAA immunocytochemistry has been used both in sections and in whole mounts to reveal a novel transverse boundary in the neonatal cerebellum that is associated with two classes of axons, a subset of climbing fiber afferents from the inferior olivary nuclei and a subset of parallel fibers, the axons of granule cells. These expression domains split the CZ into two: an anterior central zone (=CZa), which comprises lobules VIa, b of the vermis and the lobulus simplex of the hemispheres, and a central posterior zone (=CZp), which is coextensive with lobule VII and the ansiform lobules. These data therefore reveal a novel level of complexity in cerebellar topography.

EXPERIMENTAL PROCEDURES

Mice

All animal procedures conformed to institutional regulations and the *Guide to the Care and Use of Experimental Animals* from the Canadian Council for Animal Care. All experiments conformed to international guidelines on the ethical use of animals. All efforts were made to minimize the number of animals used and their

[1] Present address: Department of Anatomy, College of Medicine, Konyang University, Nosan, Chungnam 320-711, South Korea.

*Corresponding author. Tel: +1-403-220-5036; fax: +1-403-270-9497.
E-mail address: rhawkes@ucalgary.ca (R. Hawkes).

Abbreviations: AZ, anterior zone; CaBP, calbindin perinatal stripe marker; CZ, central zone; CZa, anterior central zone; CZp, central posterior zone; DAB, diaminobenzidine; HRP, horseradish peroxidase; NAA, neurofilament-associated antigen; NZ, nodular zone; P, postnatal day; PZ, posterior zone; ROR, retinoic acid orphan receptor.

0306-4522/08$32.00+0.00
doi:10.1016/j.neuroscience.2008.02.036

suffering. Three strains of mice—B6129SF2/J and C57BL/6J, and heterozygous *thy1*-YFP (line *thy1*-YFP16) mice backcrossed into C57BL/6 (Feng et al., 2000)—were obtained from Jackson Laboratories (Bar Harbor, ME, USA) and maintained in our animal facilities: no significant differences were noted between strains.

Antisera

3A10 Is a mouse monoclonal antibody that recognizes a family of NAA. It was obtained from the Developmental Studies Hybridoma Bank developed under the auspices of the National Institute of Child Health and Human Development and maintained by the University of Iowa, Department of Biological Sciences (Iowa City, IA, USA) (used diluted 1:1000). Rabbit anti-neurofilament H is a polyclonal antiserum against HPLC-purified primate phosphorylated neurofilament H (200/210 kDa: Biomol International cat. # NA1211: Linnarsson et al., 2001). Two different mouse monoclonal anti-calbindins were used, one from Sigma, St. Louis, MO, USA (anti-calbindin-D-28K, clone CB-955, ascites fluid, IgG1 isotype raised against bovine kidney calbindin: used diluted 1:1000) and the other from Swant, Bellinzona, Switzerland (McAb 300, lot #18(F): raised against chicken calbindin and specifically stains the ^{45}Ca-binding spot of calbindin D-28k (apparent molecular weight 28,000, isoelectric point 4.8) in a two-dimensional gel of mouse brain homogenate (manufacturer's information); used here diluted 1:2000). Both antibodies yielded Purkinje cell specific staining identical to that reported often before (e.g. De Camilli et al., 1984; Ozol et al., 1999). Rabbit anti-calbindin D-28K antiserum (anti-CaBP: Swant Inc., code # CB38, lot # 9.03; diluted 1:10,000) was produced against recombinant rat calbindin D-28K. In the cerebellum, CaBP is exclusively expressed in Purkinje cells (e.g. Baimbridge et al., 1982). Anti-zebrin II is a mouse monoclonal antibody produced by immunization with a crude cerebellar homogenate from the weakly electric fish *Apteronotus* (Brochu et al., 1990) and subsequently shown to bind the respiratory isoenzyme aldolase c (Aldoc: Ahn et al., 1994; Hawkes and Herrup, 1996: it was used directly from spent hybridoma culture medium diluted 1:400). Rabbit anti-phospholipase Cβ4 was raised against a synthetic peptide representing amino acids 15–74 of the mouse PLCβ4 protein fused to glutathione-S-transferase and expressed in bacteria (used diluted 1:1000). Control immunohistochemistry using either antibodies pre-absorbed with antigen polypeptides or cerebellar sections from a PLCβ4 knockout mouse yielded no significant immunostaining (Nakamura et al., 2004; Sarna et al., 2006). An identical staining pattern was also obtained with another anti-PLCβ4 antiserum, raised in guinea pig (M. Watanabe, unpublished observations). Rabbit anti-neurogranin was raised against a full-length recombinant rat neurogranin protein (Chemicon Inc., Temecula, CA, USA: catalog #AB5620; used diluted 1:5000): further details of the characterization are found in Larouche et al., 2006). Previous studies using this same antibody have shown that neurogranin-like immunoreactivity is expressed in Golgi cells of the murine cerebellum (Singec et al., 2003; Larouche et al., 2006). Goat anti-retinoic acid orphan receptor (ROR)α (1:2000, Santa Cruz Biotechnology, Santa Cruz, USA) specifically recognizes Purkinje cells, both in the adult cerebellum and during embryogenesis (Ino, 2004). Rabbit anti-Pax6 (used diluted 1:2000, Chemicon Inc.), raised against the C-terminus of murine Pax-6, specifically recognizes granule cells in the cerebellum (Engelkamp et al., 1999; Yamasaki et al., 2001).

Perfusion and sectioning

Mice were deeply anesthetized with sodium pentobarbital (100 mg/kg, i.p.) and transcardially perfused with 0.9% NaCl in 0.1 M phosphate buffer (pH 7.4) followed by 4% paraformaldehyde in 0.1 M phosphate buffer (pH 7.4). The brains were removed, post-fixed in 4% paraformaldehyde at 4 °C for 48 h. The cerebella were then cryoprotected through a series of buffered 10% (2 h), 20% (2 h), and 30% (overnight) sucrose solutions. Series of 40 μm thick transverse sections were cut through the extent of the cerebellum on a cryostat and collected in PBS for free-floating immunohistochemistry.

Immunohistochemistry

Peroxidase immunohistochemistry was carried out on cerebellar sections as described previously (Sillitoe et al., 2003). Briefly, tissue sections were washed thoroughly, blocked with 10% normal goat serum (Jackson Immunoresearch Laboratories, West Grove, PA, USA) and then incubated in 0.1 M PBS buffer containing 0.1% Triton X-100 and the primary antibody for 16–18 h at room temperature. Secondary incubation in horseradish peroxidase (HRP)–conjugated goat anti-rabbit or HRP-conjugated goat anti-mouse antibody (diluted 1:200 in PBS; Jackson Immunoresearch Laboratories) lasted 2 h at room temperature. Diaminobenzidine (DAB, 0.5 mg/ml) was used as the chromogen. Sections were dehydrated through an alcohol series, cleared, and coverslipped with Entellan mounting medium (BDH Chemicals, Toronto, ON, Canada). Cerebellar sections for double-label fluorescent immunohistochemistry were processed as described previously (Sillitoe et al., 2003). Briefly, tissue sections were washed, blocked in PBS containing 10% normal goat serum (Jackson Immunoresearch Laboratories) and incubated in both primary antibodies overnight at room temperature, rinsed, and then incubated for 2 h at RT in a mixture of Alexa 546–conjugated goat anti-rabbit Ig and Alexa 488–conjugated goat anti-mouse Ig (Molecular Probes Inc., Eugene, OR, USA), both diluted 1:2000. After several rinses in 0.1 M PBS, sections were coverslipped in non-fluorescing mounting medium (Fluorsave Reagent, Calbiochem, La Jolla, CA, USA). Whole mount peroxidase immunocytochemistry was performed according to Sillitoe and Hawkes (2002) except that the PBS containing 5% skim milk (Nestlé Foods Inc., North York, ON, Canada) plus 0.1% Triton-X 100 (Sigma) was used as blocking solution. Biotinylated goat anti-rabbit IgG (Jackson Immunoresearch Laboratories Inc.) was diluted 1:1000 in PBS containing 0.1% Triton X-100 and incubated with the cerebellum overnight. Cerebella were washed with PBS (3×2 h) and subsequently incubated overnight with ABC complex solution prepared according to the manufacturer instructions (Vectastain, Vector Laboratories Inc., Burlingame CA, USA). Antibody binding was revealed by using DAB as the chromogen.

Photomicrographs were captured with a SPOT Cooled Color digital camera (Diagnostic Instruments Inc.) and assembled in Adobe Photoshop version 9.0. For confocal microscopy, an Olympus Fluoview BX50 microscope was used running under Fluoview software. For confocal microscopy, an Olympus Fluoview BX50 microscope was used and Z-stacked images (10 layers, each 2 μm in depth) were captured by using Fluoview software. The images were cropped and corrected for brightness and contrast and montages were assembled in Adobe Photoshop 9.

RESULTS

NAA is co-expressed with anti-NF in the adult cerebellum

Neurofilaments comprise a heterogeneous group of proteins, and neurofilaments in different brain locations have differences in molecular structure (e.g. Liu et al., 2004). Fig. 1 compares the expression of NAA immunoreactivity (Fig. 1A) in the adult mouse cerebellar cortex to that of a well-characterized anti-neurofilament H antibody (Fig. 1B: Linnarsson et al., 2001). Double label immunofluorescence reveals that both antigens are strongly expressed in basket cell axons surrounding the Purkinje cell somata. In addition, NAA immunoreactivity is associated with a subset

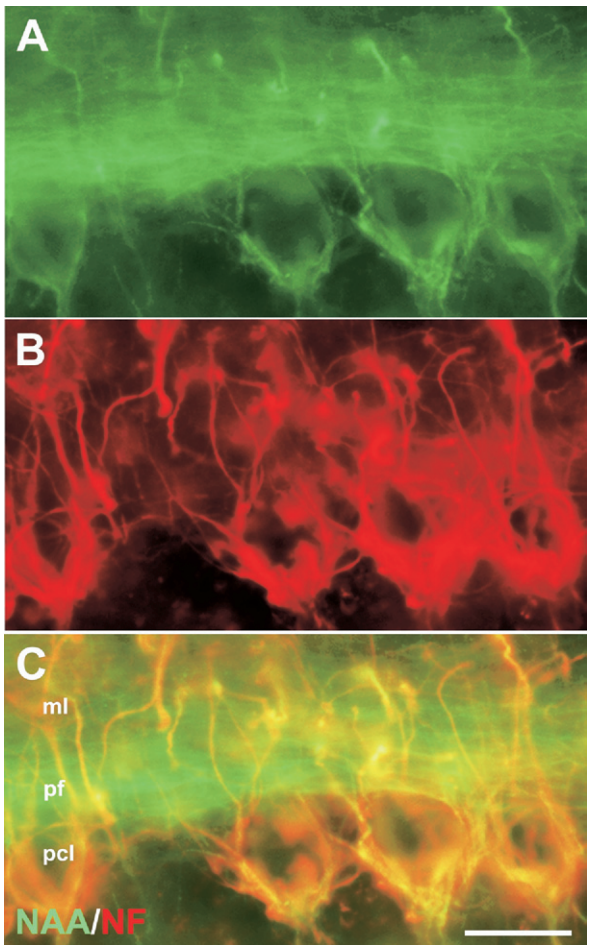

Fig. 1. Neurofilament antigens seen in transverse cryostat sections through the adult mouse cerebellar cortex. Double immunofluorescence labeling with anti-NAA (A), anti-NFH (B) and the merged image (C) shows double labeling in the basket cell axons that form the pericellular nets and pinceaux around Purkinje cell somata in the Purkinje cell layer (pcl). In addition, NAA expression is associated with parallel fibers (pf) concentrated in the deeper part of the molecular layer (ml). Scale bar=20 μm (A–C).

of parallel fibers coursing immediately above the Purkinje cells somata in the molecular layer (Fig. 1C).

NAA reveals a novel transverse boundary in the neonatal cerebellum

The topographical distribution of NAA immunoreactivity in the cerebellum at postnatal day (P) 0 is revealed by using cerebellar whole mount immunocytochemistry (Fig. 2). In the AZ no NAA immunoreactivity is detected in the vermis, but two or three, weakly NAA-immunoreactive (NAA^+) parasagittal stripes are present laterally in the paravermis and anterior lobe hemispheres (lobules III–V), which appear to extend caudally into the lobulus simplex (Fig. 2A).

The boundary in the vermis between the AZ and the CZ lies in the primary fissure between lobule V and lobule VIa (Ozol et al., 1999; Armstrong et al., 2000; Sillitoe and Hawkes, 2002; Sarna et al., 2006 etc.). The same boundary also represents a restriction boundary for NAA expression (Fig. 2A, B). In lobule V of the vermis (the posterior limit of the AZ) NAA is either weakly expressed or not present at all. In lobule VIa/b, on either side of the midline of the vermis, a pair of well-defined, strongly NAA-immunopositive stripes is found, centered ~320 μm from the midline. Seen at higher magnification, each broad stripe appears as a pair divided into two by a narrow immunonegative gap (Fig. 2B). Additional parasagittal stripes can also be discerned in the lobulus simplex of the hemispheres but these are less well defined and display weaker NAA immunoreactivity than in the vermis.

The distribution of anti-NAA immunoreactivity changes dramatically again at the posterior superior fissure be-

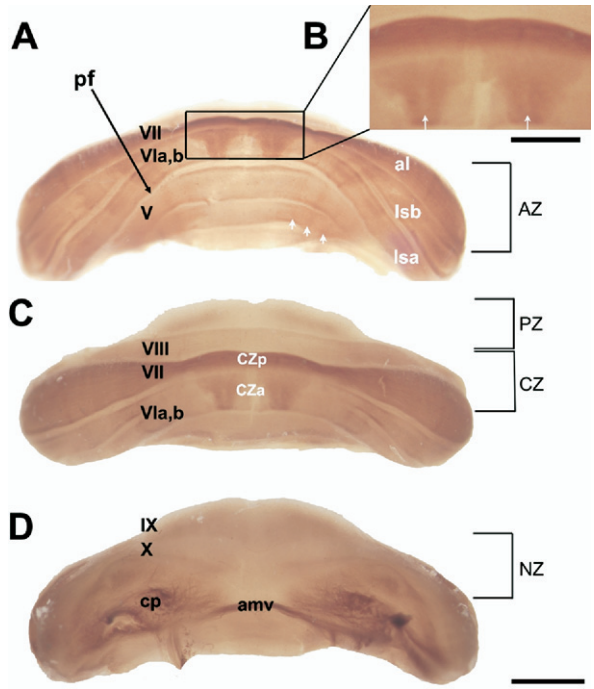

Fig. 2. Whole mount NAA peroxidase immunocytochemistry reveals a reproducible pattern of transverse zones and parasagittal stripes in the mouse cerebellum at P0. Lobules in the vermis are identified by roman numerals. (A) In an anterior view, there is no NAA-immunoreactivity in the vermis of the AZ (lobules III–V are seen), but symmetrical, weakly-immunoreactive parasagittal stripes can be seen in the lobulus simplex (lsa=lobulus simplex anterior; lsb=lobulus simplex posterior) and in the paravermian region of the anterior lobe (lobules III–IV: arrows). More caudally, a strongly immunoreactive parasagittal stripe extends on either side of the midline from the caudal face of the primary fissure (pf: between lobules V and VI) posteriorly through lobule VIa/b to the anterior boundary of lobule VII (it extends the full length of the CZ to the boundary with the PZ, but this is obscured in the CZp in whole mount views). NAA immunoreactivity in lobule VII appears uniform and strong, and extends laterally into the ansiform lobule (al). (B) A high magnification view of lobule VI, from the region outlined by the rectangle in A, to show that each NAA^+ stripe in lobule VIa comprises a doublet, separated by a narrow immunonegative gap (arrows). The same can be seen in transverse sections (see Fig. 4 below). (C) In a dorsal view, the subdivision of the CZ is clear with overt stripes in lobule VIa/b (CZa), homogeneous immunoreactivity in lobule VII (CZp: and ansiform lobule), and a uniformly immunonegative lobule VIII (anterior PZ). (D) In a ventral view, lobules IX and X (the NZ) are also NAA-immunonegative (as is lobule I, the most anterior lobule of the AZ). Abbreviations: cp=cerebellar peduncle; amv=anterior medullary vellum. Scale bars=1 mm (A, C, D); 500 μm (B).

tween lobules VIb and VII. All of lobule VII in the vermis, together with its lateral extensions—the ansiform lobules of the hemispheres (crus I and crus II are not distinct in the newborn mouse)—comprises a uniformly and strongly NAA-immunopositive expression domain (Fig. 2A, C). No stripes are apparent in the whole-mount staining, as they are obscured by the overlying homogeneous immunoreactivity, but in sections it is clear that they extend the full length of the CZ (see below). The staining pattern changes again in the prepyramidal fissure between lobules VII and VIII, which also represents the boundary between the CZ and the PZ (Fig. 2C). Caudal to the prepyramidal fissure the strong anti-NAA staining in the posterior CZ is replaced by no immunoreactivity in the PZ (e.g. lobule VIII: Fig. 2C) and the NZ (e.g. lobule X: Fig. 2D).

Thus, the novel result is that the CZ (=lobules VI and VII in the vermis; the lobulus simplex and the ansiform lobule in the hemispheres) is apparently subdivided by the expression pattern of NAA into two transverse expression domains: in whole mount these appear as a striped CZa comprising lobules VIa/b and the lobulus simplex and a uniform CZp comprising lobule VII and the ansiform lobules.

The developmental profile of NAA staining

NAA-immunoreactivity is first expressed in the cerebellar primordium as early as E8/9 (Doorn et al., unpublished observations) but the differential expression that distinguishes CZa from CZp is restricted to the period of the E17 to P7 (Fig. 3). At older ages, NAA-immunoreactivity spreads to other lobules (Fig. 3) and in the adult the distribution is dominated by parallel fibers and basket cell axons (Fig. 1).

The expression of NAA during developmental varies between transverse zones. In the AZ no expression is detected before P7: later, weak stripes of immunoreactivity are found that persist into adulthood (data not shown). Striped NAA expression in the CZa (lobule VIa/b) emerges at ~E17 with strong immunoreactivity both in the vermis and hemispheres (Fig. 3A). These stripes are clearly recognizable until ~P8 after which they disappear. Uniform expression in the CZp is present from E17 as a narrow transverse fiber bundle. At E17 this narrow fascicle is restricted to the putative lobule VIb/VII boundary but broadens to the edge of the VII/VIII boundary to occupy all the CZp, vermis and hemispheres, by P0 (Fig. 3B). This fascicle preceded any sign of formation of the sulcus separating VIa/b from VII (the posterior superior fissure). The CZp remains distinct until P5 (Fig. 3C), after which time immunoreactivity increases in the other lobules and concomitantly has weakened in CZp, so that by P8 (Fig. 3D) the distinct CZp is no longer apparent. Finally, although there are sometimes signs of very weak NAA^+ stripes in the PZ/NZ, these are not stained reliably and we have treated these two zones as immunonegative throughout development (e.g. Fig. 2D). The same stripe array is also seen in transverse sections through the CZa of the developing cerebellum immunoperoxidase stained by using 3A10 (P0, Fig. 4A; P3, Fig. 4B). In contrast, antisera against phosphorylated epitopes on the 200 kDa neurofilament subunit (SMI31, e.g. Sternberger and Sternberger, 1983; anti-neurofilament H, Linnarsson et al., 2001) give uniform staining, and immunoreactivity for non-phosphorylated neurofilament epitopes on NFH (SMI32: e.g. Sternberger and Sternberger, 1983; Dusart et al., 1997) is absent (data not shown). Thus the differential expression

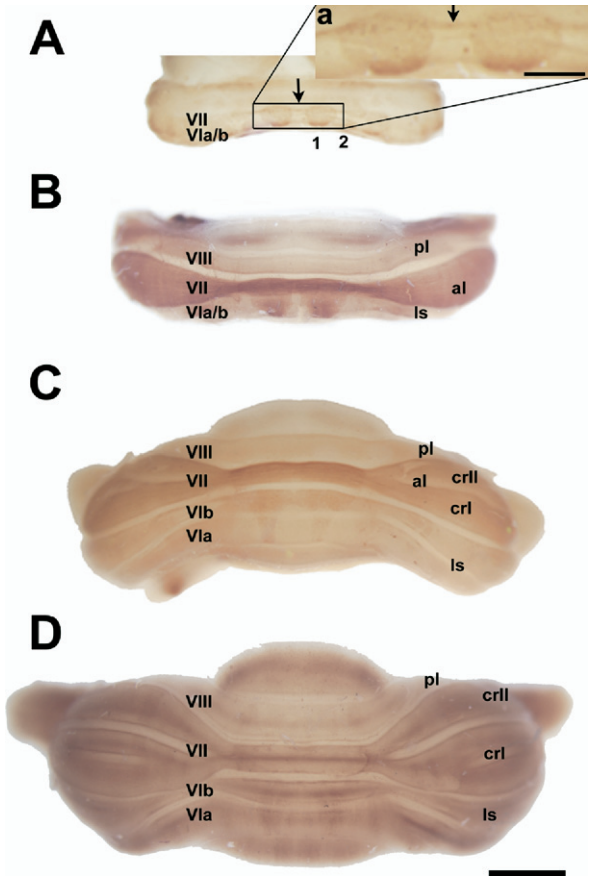

Fig. 3. The perinatal development of NAA expression in the cerebellum as revealed by whole mount peroxidase immunocytochemistry (dorsal views). Lobules in the vermis are indicated by roman numerals. (A) NAA immunohistochemistry at E17 reveals a stripe array in the vermis of lobules VI/VII (CZ) and the nascent lobulus simplex in the hemispheres. One pair of stripes is situated in the vermis ~280 μm either side of the midline (1) with a second pair located ~750 μm from the midline in the hemispheres (2). In addition, a narrow NAA^+ fiber fascicle runs along the edge of the prepyramidal sulcus between lobules VII and VIII (arrow). The pair of stripes adjacent to the midline is shown at higher magnification in the inset (a). (B) At P0, the stripe array in the CZa is still prominent. In addition uniform immunoreactivity has expanded to occupy all lobule VII in the vermis (the CZp), and the entire nascent ansiform lobule of the hemispheres (al: the intrahemispheric fissures are still immature and crus I and II are fused). (C) By P5 the NAA-immunoreactivity in the CZa stripe array has begun to fade. In the CZp, immunoreactivity is still prominent. In the hemispheres, the intrahemispheric fissure has appeared in the ansiform lobule between crus I (crI) and crus II (crII), and the higher staining intensity differentiates the ansiform lobule from the neighboring lobulus simplex (ls) and paramedian lobule (pl). (D) By P8, the stripe array in the CZa is weak, and the anti-NAA staining intensity has increased in other parts of the cerebellum such that a distinct CZp can no longer be discerned. Parasagittal stripes can still be seen in the CZa (lobule VIa, b). Scale bars=1 mm (A–D); 250 μm (inset a).

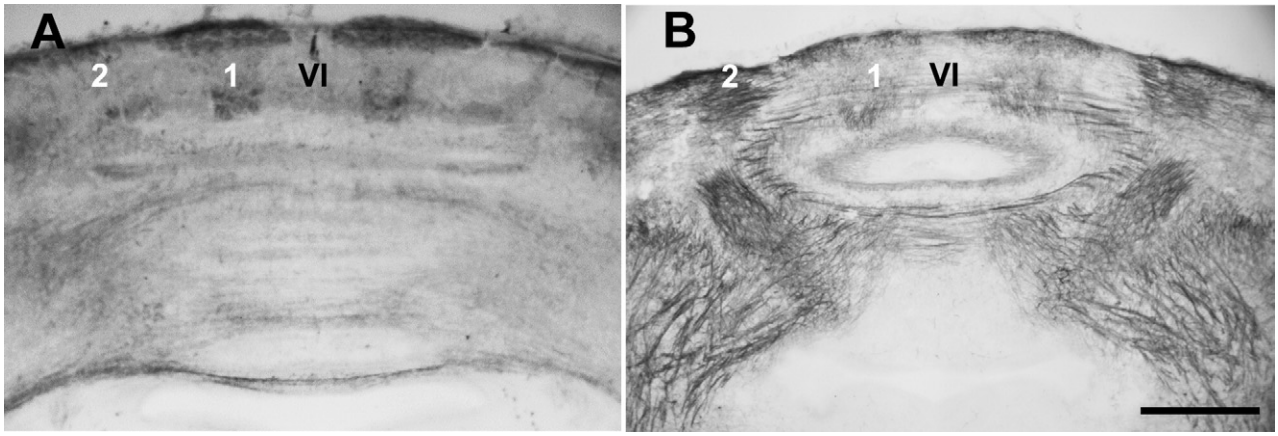

Fig. 4. NAA peroxidase immunocytochemistry of 40 μm cryostat transverse sections through lobule VI of the cerebellar vermis at P0 (A) and P3 (B) showing two parasagittal stripes of expression (1, 2) in the CZa. As in the whole mount views (e.g. Fig. 2B), these stripes sometimes present as doublets. Scale bar=500 μm (A, B).

pattern is not characteristic of neurofilament antigens in general.

What is the structural basis of NAA stripes in the CZ?

There are three plausible candidates for the NAA$^+$ stripes in the CZ, each of which is already known to be organized in stripes in the perinatal cerebellum: climbing fibers, mossy fibers (reviewed in Sotelo and Wassef, 1991; Sotelo and Chédotal, 2005) and Purkinje cell dendrites (reviewed in Herrup and Kuemerle, 1997; Armstrong and Hawkes, 2000; Larouche and Hawkes, 2006 etc.). The evidence does not support the hypothesis that these are mossy fiber stripes. Mossy fibers terminate in the granular layer in the adult (Fig. 5A). In the embryonic and perinatal cerebellum they form direct contacts with Purkinje cell somata but rarely extend superficially into the molecular layer (Fig. 5B). Instead, they are displaced into the granular layer as granule cells migrate from the external granular layer. The NAA$^+$ axons clearly extend beyond the Purkinje cells into the developing molecular layer (Fig. 5C). This can be compared with the distribution of mossy fibers, as revealed by the expression of a *thy1*-YFP transgene (Feng et al., 2000). First, there is no co-expression of *thy1*-YFP and NAA (Fig. 5Dd). Next, NAA$^+$ axons clearly extend into the molecular layer, past the Purkinje cells (Fig. 5C: and sometimes perisomatic; for example inset Fig. 5Cc), while the mossy fibers are confined to the immature granular layer (Fig. 5B). Similarly, the immunoreactivity is not associated with Purkinje cells. CaBP in the cerebellum is expressed only in Purkinje cells (e.g. De Camilli et al., 1984). Double immunofluorescence labeling for CaBP and NAA reveals no co-expression (although the profiles are intermingled: Fig. 5C). Therefore, we hypothesize that these stripes represent a specific subset of climbing fiber axons. We see no staining in the source of the climbing fibers: the inferior olivary complex (data not shown).

In sagittal views, the NAA-immunopositive axon projection (green) can be followed through the cerebellum to a distinct terminal field in the CZ (Fig. 6A, B). It is restricted rostrally in the nascent lobule VIa, b on the caudal face of the primary fissure (the same place that the AZ and CZ interdigitate: Ozol et al., 1999). Caudally it ends abruptly at a boundary at which the prepyramidal fissure will form between lobules VII and VIII (Fig. 6A, B).

Marani and Voogd (1979) identify a gap in the molecular layer in this region in the adult mouse, and Pax6 immunostaining (an antigenic marker of the external granular layer and developing granule cells: Swanson et al., 2005) shows a reproducible thinning of the external granular layer in this region (Fig. 6A, B). Interestingly, this region of the superficial cortex is also different in that the Purkinje cells are less-well organized into a monolayer: for example, at E18 immunoperoxidase staining using the Purkinje cell marker RORα (Ino, 2004) reveals a discontinuity in the Purkinje cell layer at same site (Fig. 6C, D). It is clear that this transverse boundary predates the formation of the prepyramidal fissure between lobules VII and VIII and also precedes NAA expression. Sections through the vermis immunoperoxidase stained for Pax6 reveal the zone of thinned EGL as early as E15 (Fig. 6E), which is clearly evident at E16 (Fig. 6F), E18 (Fig. 6G) and P3 (Fig. 6H).

The topography of the NAA stripes can be related to those of antigens described previously. Most adult stripe antigens are not expressed in the temporal window during which the CZa and CZp can be distinguished (e.g. zebrin I, Hawkes and Leclerc, 1987; zebrin II, Lannoo et al., 1991; others do not show stripes in the perinatal CZ, e.g. HSP25, Armstrong et al., 2001; neurogranin, Larouche et al., 2006). A notable exception is phospholipase Cβ4, which is expressed in a family of (zebrin II-immunonegative) stripes that is consistent throughout postnatal development (Marzban et al., 2007) and into adulthood (Sarna et al., 2006). Although all Purkinje cells in the CZ are zebrin II-immunopositive/PLCβ4-immunonegative, stripes are clear at the zone boundaries where the CZ interdigitates with the neighboring AZ and PZ. In these regions it is possible to compare NAA stripes to the Purkinje cell compartmenta-

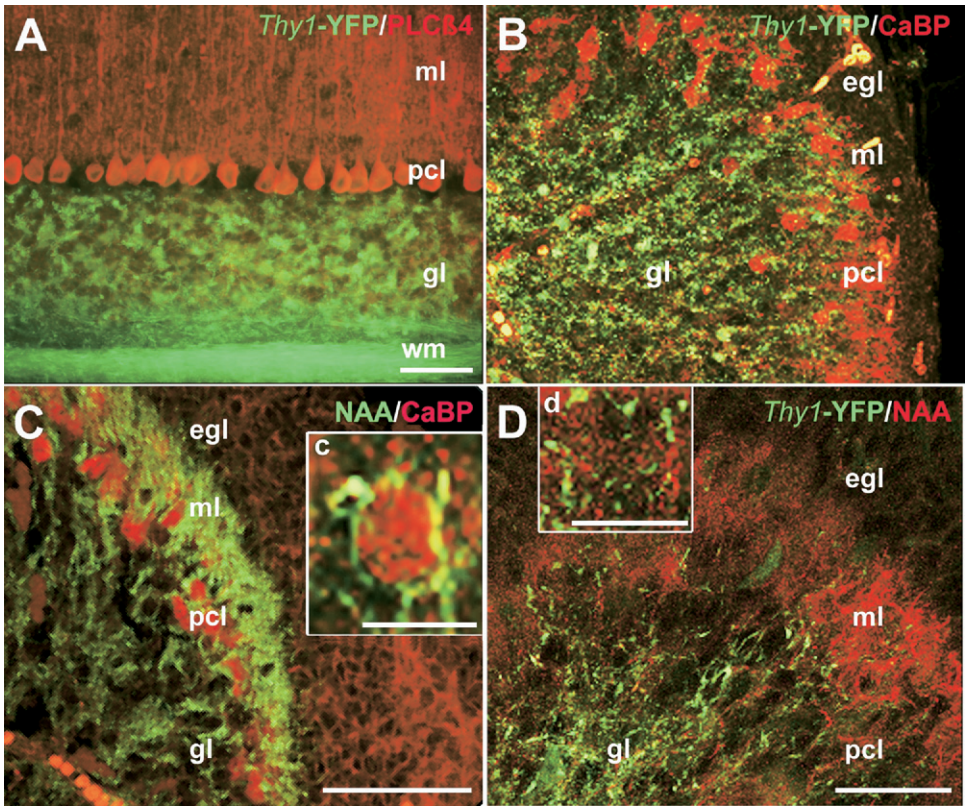

Fig. 5. Stripes of NAA immunoreactivity in the developing CZa are neither associated with mossy fibers nor Purkinje cells. (A) In transverse sections through the adult cerebellum a *thy1*-YFP transgene (green) is expressed in mossy fibers. The fluorescence is seen in mossy fiber axons of the white matter tracts (wm), which terminate in synaptic glomeruli in the granular layer (gl) but do not extend through the Purkinje cell layer (pcl) into the molecular layer (ml: Purkinje cell dendrites are immunofluorescence stained by using anti-PLCβ4, red; Sarna et al., 2006). (B) In a confocal image of a sagittal section through the P3 cerebellum, mossy fiber axons that express the *thy1*-YFP transgene (green) are restricted to the immature granular layer and Purkinje cell multilayer (pcl: anti-CaBP, red), and rarely extend beyond into the molecular layer. (C) A confocal image of a sagittal section through the P3 cerebellum. In contrast to the mossy fibers, NAA^+ axons at P3 (green) extend well beyond the Purkinje cell multilayer (pcl: revealed by using anti-CaBP, red) to reach the immature molecular layer. They terminate beneath the external granular layer (egl). There is no co-expression of NAA and CaBP. (c) At a higher magnification NAA^+ axons terminal are seen surrounding the Purkinje cell somata. (D) A confocal image of a 40 μm sagittal section through the cerebellar vermis of a *thy1*-YFP transgenic mouse (green) at P3, immunofluorescence stained for NAA (red), reveals no co-expression: *thy1*-YFP-expressing mossy fibers are restricted to the granular layer (gl) and white matter tracts; NAA^+ axons extend into the molecular layer (ml). The inset (d) shows tissue from the same region at a higher magnification. Scale bars=50 μm (A); 50 μm (C); 50 μm (B, D); 10 μm (inset c); 20 μm (inset d). For interpretation of the references to color in this figure legend, the reader is referred to the Web version of this article.

tion. For example, the rostral extensions of the NAA^+ stripes from VIb to VIa are clearly PLCβ4-immunonegative with sharp and well-define boundaries (Fig. 7A, B, D–F). A second perinatal stripe marker is calbindin (CaBP). CaBP is expressed in the adult cerebellum in all Purkinje cells and no other cells are immunoreactive (e.g. Baimbridge and Miller, 1982). However, in the perinatal cerebellum, CaBP expression is transiently restricted to a Purkinje cell subset that forms a reproducible stripe array (rat, Wassef et al., 1985; mouse, Ozol et al., 1999). When NAA and CaBP are compared the cluster of midline Purkinje cells that strongly express CaBP in lobule VI is restricted to the NAA-immunonegative stripe, while NAA-immunopositive stripes overlap with weakly CaBP-immunopositive Purkinje cells more laterally (Fig. 7C). Finally, neurogranin is a Purkinje cell stripe marker in the perinatal cerebellum (Larouche et al., 2006). The neurogranin stripe array aligns with that revealed by anti-NAA staining (Fig. 7G–I), although the same structures are not co-labeled (anti-NAA labels axons; neurogranin is expressed in Purkinje cells: see Fig. 5C).

What is the structural basis of uniform NAA staining in the CZp?

As seen by using whole mount NAA immunohistochemistry the intense uniform NAA-immunoreactivity in lobule VII is localized to a bundle of fibers running parallel to the long axis of the folia (Fig. 8A). The fibers can also be seen in sections (sagittal, Fig. 8B; transverse, Fig. 8C). The bundle is situated superficially on the cerebellar cortex, external to the Purkinje cells (Fig. 8B, C), sandwiched between the Purkinje cells and the external granular layer (Fig. 8B, C). Therefore, we conclude that the homogeneous fiber bundle immunostaining in the CZp is associated with a specific population of parallel fiber axons. This is consistent with the NAA expression pattern in the adult cerebellum (Fig. 1), which also shows parallel fiber immunoreactivity. Also con-

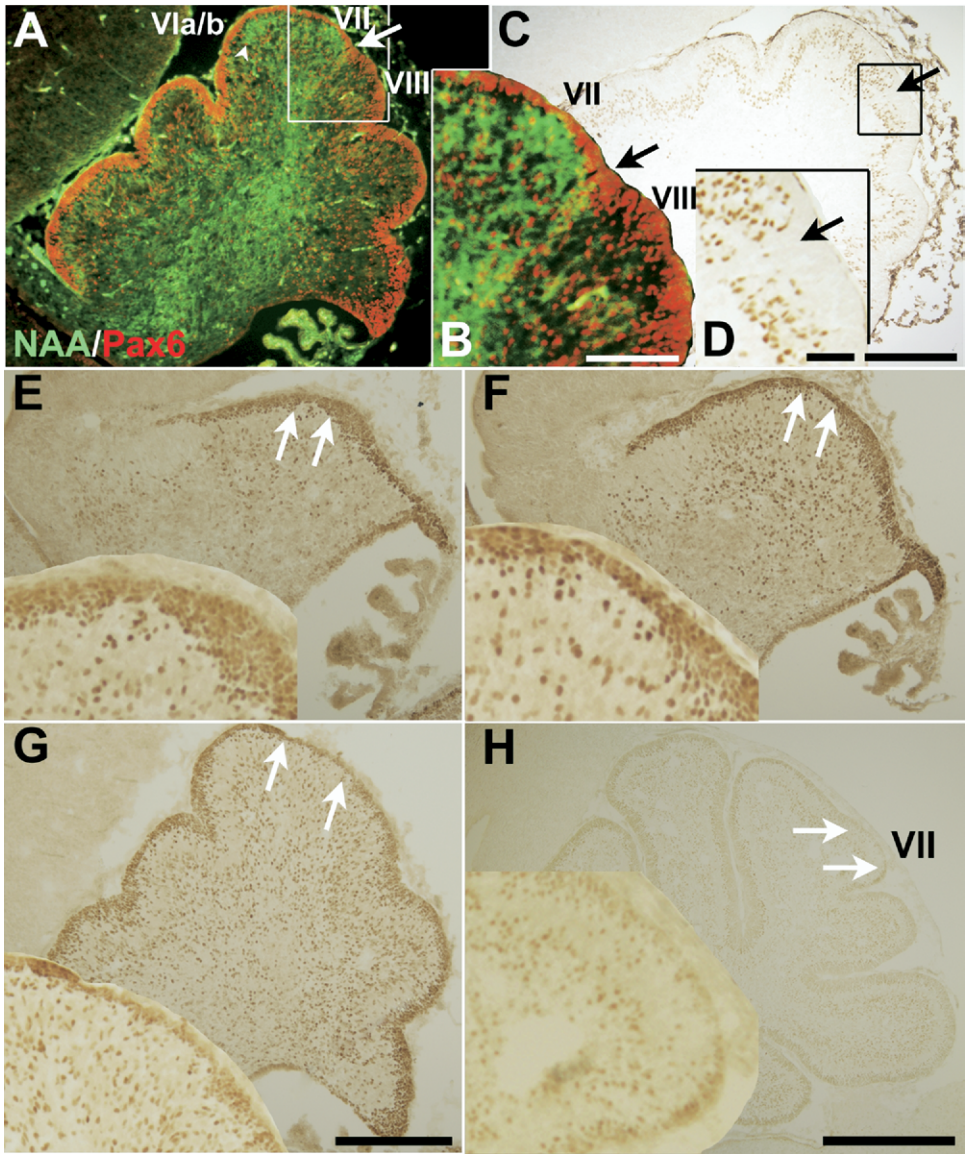

Fig. 6. (A, B) The NAA$^+$ putative climbing fibers in the CZ can be followed in sagittal sections at E18 immunostained for NAA and Pax6. Pax6 is a marker of the external granular layer and developing granule cells. A sagittal section through the cerebellum at E18 double immunofluorescence stained for Pax6 (red) and NAA (green) shows the NAA$^+$ climbing fiber projection to the CZ. The terminal field begins rostrally in the caudal face of the primary fissure (arrowhead), extends through nascent lobules VI/VII and forms a sharp boundary caudally in the vermis where the prepyramidal fissure will form between lobules VII and VIII (the CZ/PZ boundary: indicated by a slight indentation of the cortical surface; arrow). Note that the external granular layer over the CZp is thinner than over neighboring zones. (C, D) Sagittal views of the E18 mouse cerebellum immunoperoxidase stained for RORα, a specific marker of embryonic Purkinje cells (Ino, 2004). A gap is present in the Purkinje cell multilayer (arrow), which corresponds to the caudal restriction boundary for the NAA$^+$ climbing fiber projection. (E–H) A thinning of the external granular layer over the region of the cerebellum that will become lobule VII in the vermis can be traced in sagittal sections through the vermis immunoperoxidase-stained for Pax6. The region of thinned EGL is indicated by arrows and shown at higher magnification in the insets, and is seen as early as E15 (E), E16 (F), E18 (G) and P3 (H). Scale bars=100 μm (B); 250 μm (A, C); 100 μm (D); 250 μm (E–G); 500 μm (H). For interpretation of the references to color in this figure legend, the reader is referred to the Web version of this article.

sistent with this interpretation, double immunofluorescence staining with anti-NAA and anti-Pax6 revealed that a small subset of granule cells in the granular layer also is NAA-immunopositive (Fig. 8D, E).

DISCUSSION

The Purkinje cells of the CZ have three distinguishing features: all are zebrin II$^+$, all are PLCβ4$^-$, and there is a stripe array revealed by expression of HSP25. Until now, despite minor complications due to interdigitating stripes from neighboring zones, there has been no reason to think that the CZ was not a single zone. In particular, previous studies of expression patterns reveal no evidence of a difference between lobules VI and VII (e.g. zebrin II, all Purkinje cells are immunopositive (e.g. Ozol et al., 1999; Sillitoe and Hawkes, 2002); PLCβ4, all are immunonegative

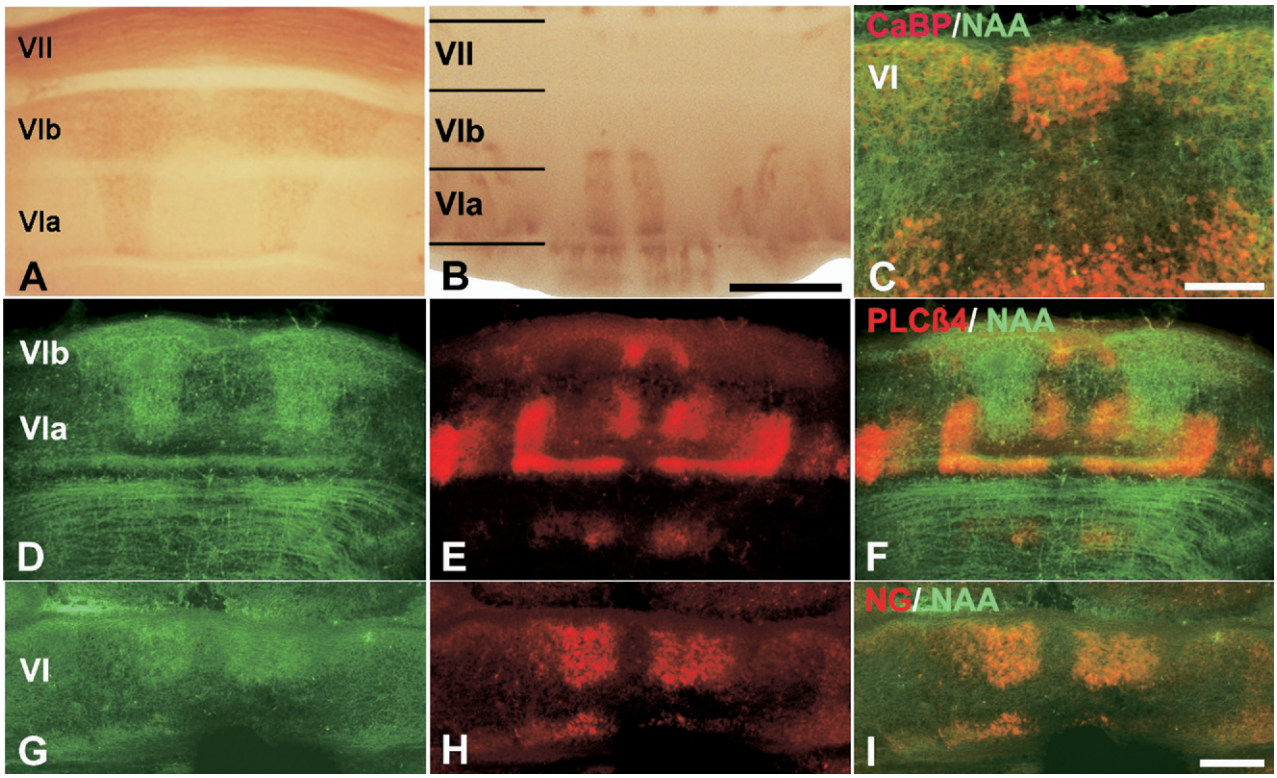

Fig. 7. The stripe topography of the NAA$^+$ putative climbing fiber projection. (A) Whole mount NAA immunostaining of the CZ at P5 showing striped expression in the CZa (lobules VIa, b) and uniform expression in the CZp (lobule VII). (B) Whole mount PLCβ4 immunostaining of the CZ at P5 showing Purkinje cell stripes in lobule VIa. These are the posterior extensions of the P1$^-$ stripes of the AZ (for more details and stripe terminology, see Marzban et al., 2007). (C) Transverse section through lobule VI at P0 double immunofluorescence labeled for CaBP (red) and NAA (green) shows a midline cluster of Purkinje cells that strongly expresses CaBP with weak CaBP expression in the neighboring stripes. The NAA$^+$ axons ramify throughout the weakly-CaBP immunoreactive clusters but not in the strongly immunoreactive medial cluster. (D–F) Transverse section through lobule VI double immunofluorescence at P4 stained for NAA (D), PLCβ4 (E), and the merged image of D and E (F) reveals that NAA$^+$ axons terminate preferentially in PLCβ4-immunonegative Purkinje cell stripes. (G–I) Transverse section through lobule VI double immunofluorescence at E18 labeled for NAA (G), neurogranin (H), and the merged image of G and H (I). The NAA$^+$ axons terminate in the neurogranin-immunoreactive stripes, although within the terminal field, neurogranin and NAA are not co-expressed. Scale bars=500 μm (A, B); 100 μm (C); 100 μm (D–I). For interpretation of the references to color in this figure legend, the reader is referred to the Web version of this article.

(Sarna et al., 2006); HSP25, continuous stripes of expression extend uninterrupted across VI and VII (adult, Armstrong et al., 2000: all Purkinje cells in the CZ are HSP25$^-$ in the neonate, Armstrong et al., 2001); L7-pcp2-lacZ, all negative in the adult, all positive in the neonate, Ozol et al., 1999 etc.). The present data, however, point to a hitherto unappreciated, reproducible subdivision of the CZ into an anterior portion—the CZa—characterized in whole mount NAA immunocytochemistry by stripes of climbing fiber terminals, and a posterior portion—the CZp—distinguished by a unique set of parallel fibers. Such a distinction between lobules VI and VII is commonly drawn in human anatomy: the declive (=lobule VI in mouse) and hemispheric posterior quadrangular lobule are grouped together as the lobulus simplex (to reflect that there is no clear separation of vermis and hemispheres), and are distinct from the more caudal lobules of vermis; the folium and tuber and hemispheric semilunar lobules (=lobule VII+ansiform lobules).

Evidence for stripes of climbing fiber terminals comes primarily from anterograde tracing studies. There are also reports of stripes of climbing fibers that express particular antigenic markers, both in the neonate (e.g. Wassef et al., 1992a,b) and the adult (e.g. corticotropin releasing factor: King et al., 1997). In some cases, climbing fiber terminal field stripes have been shown to align with stripes of Purkinje cells (Gravel et al., 1987; Wassef et al., 1992a,b: Apps, Voogd et al., 2003; Pijpers et al., 2006; Sugihara and Quy, 2007 etc.).

Climbing fiber growth cones first enter the cerebellum at around E15 (Paradies and Eisenman, 1993), where they contact the embryonic Purkinje cell clusters, thereby establishing the olivocerebellar topography. Immunocytochemical studies have revealed ordered climbing fiber projections from E15 (Paradies and Eisenman, 1993: reviewed in Sotelo and Chédotal, 2005). This distinction disappears along much the same timelines as do the stripes of NAA expression. Although the whole mount appearance seems to restrict the climbing fiber projection to the CZa (e.g. Fig. 2), sagittal sections through the CZ reveal NAA$^+$ climbing fibers with terminal fields that extends throughout lobule VII but do not significantly enter lobule VIII (i.e. restriction rostral to the CZ/PZ boundary: Ozol et al., 1999: Fig. 6). The notion that the climbing fiber

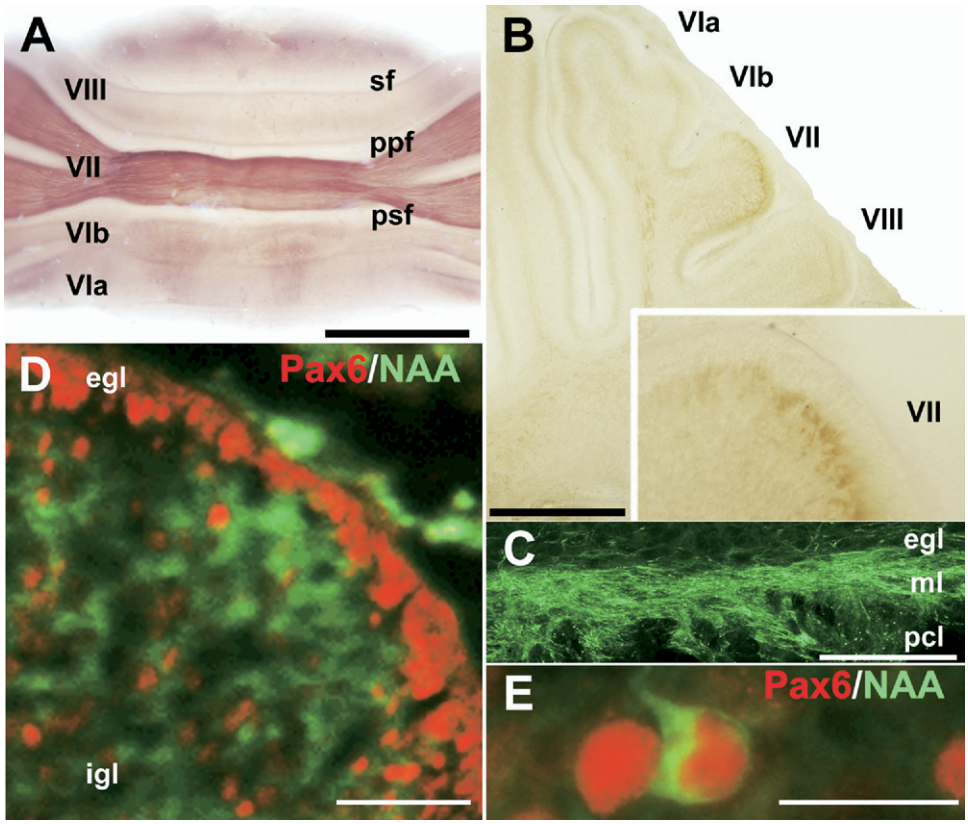

Fig. 8. Expression of NAA in parallel fiber axons of lobule VII (CZp) in the postnatal cerebellum. (A) In whole mount, the intense uniform NAA immunoreactivity in lobule VII is localized to a bundle of fibers running parallel to the long axis of the folia. (B) A 200 μm thick sagittal slice through the vermis at P5 immunoperoxidase stained by using anti-NAA. Immunoreactive axons can be seen in the white matter tract leading to lobules VI/VII and reaction product is also deposited in the immature molecular layer of lobule VII (inset). (C) A transverse section through the transverse bundle immunofluorescence stained for NAA. The confocal image reveals it to be composed of fine axonal processes concentrated in the immature molecular layer (ml), sandwiched between the Purkinje cell layer (pcl) and the superficial external granular layer (egl). (D, E) Double immunofluorescence staining of a sagittal section through lobule VII for Pax6 (red) and NAA (green). Pax6 expression is seen in both the external granular layer (egl) and in granule cells in the immature granular layer (igl). In most cases, the Pax6 and NAA immunoreactivities do not overlap. However, occasional granule cell somata are double labeled: there does not appear to be any topographical restriction to their mediolateral distribution. Abbreviations: psf=posterior superior fissure; ppf=prepyramidal fissure; sf=secondary fissure. Scale bars=1 mm (A) 500 μm (B); 50 μm (C); 25 μm (D); 20 μm (E). For interpretation of the references to color in this figure legend, the reader is referred to the Web version of this article.

topography is not restricted at the CZa/CZp boundary is consistent with previous anterograde mapping studies that show no discontinuities in the region (e.g. Voogd and Ruigrok, 2004; Sugihara and Quy, 2007).

The data reveal a distinct expression domain for NAA that is associated with a subset of parallel fibers, restricted to the CZp in lobule VII of the vermis and its hemispheric extensions as the ansiform lobules. Several possible explanations for this finding can be advanced. First, we can postulate a distinct granule cell population associated with CZp. There is substantial evidence for multiple granule cell sub types (e.g. nNOS is expressed in topographically ordered clusters and stripes of granule cells, Schilling et al., 1994; Hawkes and Turner, 1994; Sillitoe et al., 2003 etc; NMDA receptor subunit NR2C-lacZ transgene is expressed in stripes of granule cells in the immature granular layer, Karavanova et al., 2007; reviewed in Ozol and Hawkes, 1997). However, clonal analysis of granule cells in murine x-inactivation chimeras provides no evidence of a lineage restriction boundary in lobule VII (Hawkes et al., 1999). It therefore seems more plausible that differential NAA expression by a granule cell subset is secondary to its local environment. First, this could be an interaction between granule cells and their local Purkinje cell population. Alternatively, granule cells may modulate their expression patterns in response to their afferent input from mossy fibers: for example, there is evidence that the neuronal nitric oxide synthase expression by granule cell subsets is modulated by mossy fiber input (Schilling et al., 1994; Baader and Schilling, 1996). In either case, a reproducible topographical pattern of expression might be expected. Because parallel fibers can be very long (e.g. Brand et al., 1976; Mugnaini, 1983) it is not possible to determine which granule cells in the CZp express early NAA immunoreactivity. The occasional NAA^+ granule cell somata we observe (e.g. Fig. 8D, E) show no obvious stripe restriction.

The evidence that the EGL is unusually thin over lobule VII as early as E15 suggests that the unique features of parallel fibers in the lobulus simplex may pre-date afferent input. Several markers reveal differences between EGL subpopulations (e.g. Otx1/2, Frantz et al., 1994; reviewed

in Ozol and Hawkes, 1997; receptor protein tyrosine phosphatase and acidic fibroblast growth factor, McAndrew et al., 1998). None is specific to lobule VII. Furthermore, the reason that the EGL is thin over lobule VII is unclear. There is no evidence that the thin EGL (and early parallel fiber NAA expression) is due to the early maturation of this region as a whole; on the contrary, the Purkinje cells here are among the last to settle into a monolayer (see Fig. 6C, D: Vastagh et al., 2005 etc.). Likewise, it is not simple to relate the morphology of the EGL to that of the underlying Purkinje cells. There is no evidence that the Purkinje cell populations are different between CZa and CZp (e.g. HSP25, Armstrong et al., 2000; zebrin II, Sillitoe and Hawkes, 2002; PLCβ4, Sarna et al., 2006 all show no discontinuity). Thus, if the early NAA expression in the CZp is a reflection of the underlying Purkinje cell environment, why is it not seen in lobules VIa, b as well? The one exception to the idea that the Purkinje cell stripes are homogeneous through the whole CZ is the expression of Eph receptors and ephrins in transverse bands in the perinatal cerebellum that correspond to presumptive lobules (Rogers et al., 1999). In particular, expression of EphA3 and EphA5 receptors delineates the presumptive VII. The cellular substrate is presumably the Purkinje cells, but this is not certain.

CONCLUSION

In conclusion, these data indicate that there are more transverse boundaries in the cerebellum than have been appreciated. In support of this general notion, we recently reported a fifth transverse zone—the lingular zone—that is unique to birds (pigeon, Pakan et al., 2007; hummingbird, Iwaniuk et al., 2007; chicken, Marzban et al., manuscript in preparation), in which zebrin II/PLCβ4 expression distinguishes lobule I (the lingula) from the AZ (lobules II–V). Several investigators have noted that hypoplasia of lobule VI is characteristic of patients with autism (e.g. reviewed in Courchesne et al., 2004): the present identification of a unique transverse zone in this region therefore also takes on potential clinical implications.

Acknowledgments—These studies were supported by grants from the Canadian Institutes of Health Research (R.H.) and the University of Calgary URGC (H.M.).

REFERENCES

Ahn AH, Dziennis S, Hawkes R, Herrup K (1994) The cloning of zebrin II reveals its identity with aldolase C. Development 120:2081–2090.

Akintunde A, Eisenman LM (1994) External cuneocerebellar projections and Purkinje cell zebrin II bands: a direct comparison of parasagittal banding in the mouse cerebellum. J Chem Neuroanat 7:75–86.

Apps R, Garwicz M (2005) Anatomical and physiological foundations of cerebellar information processing. Nat Rev Neurosci 6:297–311.

Armstrong C, Hawkes R (2000) Pattern formation in the cerebellar cortex. Biochem Cell Biol 78:551–562.

Armstrong C, Krueger-Naug AM, Currie WC, Hawkes R (2000) Constitutive expression of the 25kDa heat shock protein Hsp25 reveals novel parasagittal bands of Purkinje cells in the adult mouse cerebellar cortex. J Comp Neurol 416:383–397.

Armstrong C, Krueger-Naug AM, Currie WC, Hawkes R (2001) Expression of heat-shock protein Hsp25 in mouse Purkinje cells during development reveals novel features of cerebellar compartmentation. J Comp Neurol 429:7–21.

Baader SL, Schilling K (1996) Glutamate receptors mediate dynamic regulation of nitric oxide synthase expression in cerebellar granule cells. J Neurosci 16:1440–1449.

Baimbridge KG, Miller JJ (1982) Immunohistochemical localization of calcium-binding protein in the cerebellum, hippocampal formation and olfactory bulb of the rat. Brain Res 245:223–229.

Brand S, Dahl AL, Mugnaini E (1976) The length of parallel fibers in the cat cerebellar cortex. An experimental light and electron microscopy study. Exp Brain Res 26:39–58.

Brochu G, Maler L, Hawkes R (1990) Zebrin II: a polypeptide antigen expressed selectively by Purkinje cells reveals compartments in rat and fish cerebellum. J Comp Neurol 291:538–552.

Chockkan V, Hawkes R (1994) Functional and antigenic maps in the rat cerebellum: zebrin compartmentation and vibrissal receptive fields in lobule IXa. J Comp Neurol 345:33–45.

Courchesne E, Redcay E, Kennedy DP (2004) The autistic brain: birth through adulthood. Curr Opin Neurol 17:489–496.

De Camilli P, Miller PE, Levitt P, Walter U, Greengard P (1984) Anatomy of cerebellar Purkinje cells in the rat determined by a specific immunohistochemical marker. Neuroscience 11:761–817.

Dusart I, Airaksinen MS, Sotelo C (1997) Purkinje cell survival and axonal regeneration are age dependent: an in vitro study. J Neurosci 17:3710–3726.

Eisenman LM, Hawkes R (1993) Antigenic compartmentation in the mouse cerebellar cortex: Zebrin and HNK-1 reveal a complex, overlapping molecular topography. J Comp Neurol 335:586–605.

Engelkamp D, Rashbass P, Seawright A, van Heyningen V (1999) Role of Pax6 in development of the cerebellar system. Development 126:3585–3596.

Feng G, Mellor RH, Bernstein M, Keller-Peck C, Nguyen QT, Wallace M, Nerbonne JM, Lichtman JW, Sanes JR (2000) Imaging neuronal subsets in transgenic mice expressing multiple spectral variants of GFP. Neuron 28:41–51.

Frantz GD, Weimann JM, Levin ME McConnell SK (1994) *Otx1* and *Otx2* define layers and regions in developing cerebral cortex and cerebellum. J Neurosci 14:5725–5740.

Gao W, Chen G, Reinert KC, Ebner TJ (2006) Cerebellar cortical molecular layer inhibition is organized in parasagittal zones. J Neurosci 26:8377–8387.

Gravel C, Eisenman LE, Sasseville R, Hawkes R (1987) Parasagittal organization of the rat cerebellar cortex: a direct correlation between antigenic Purkinje cell bands revealed by mabQ113 and the organization of the olivocerebellar projection. J Comp Neurol 263:294–310.

Gravel C, Hawkes R (1990) Parasagittal organization of the rat cerebellar cortex: direct comparison of Purkinje cell compartments and the organization of the spinocerebellar projection. J Comp Neurol 291:79–102.

Hallem JS, Thompson JH, Gundappa-Sulur G, Hawkes R, Bjaalie JG, Bower JM (1999) Spatial correspondence between tactile projection patterns and the distribution of the antigenic Purkinje cell markers anti-zebrin I and anti-zebrin II in the cerebellar folium crus IIA of the rat. Neuroscience 93:1083–1094.

Hawkes R, Beirebach E, Tan SS (1999) Granule cell dispersion is restricted across transverse boundaries in mouse chimeras. Eur J Neurosci 11:3800–3808.

Hawkes R, Herrup K (1996) Aldolase C/zebrin II and the regionalization of the cerebellum. J Mol Neurobiol 6:147–158.

Hawkes R, Leclerc N (1987) Antigenic map of the rat cerebellar cortex: the distribution of parasagittal bands as revealed by a monoclonal anti-Purkinje cell antibody, mabQ113. J Comp Neurol 256:29–41.

Hawkes R, Turner RW (1994) Compartmentation of NADPH-diaphorase activity in the mouse cerebellar cortex. J Comp Neurol 346:499–516.

Herrup K, Kuemerle B (1997) The compartmentalization of the cerebellum. Annu Rev Neurosci 20:61–90.

Ino H (2004) Immunohistochemical characterization of the orphan nuclear receptor ROR alpha in the mouse nervous system. J Histochem Cytochem 52:311–323.

Iwaniuk AN, Hawkes R, Marzban H, Pakan JMP, Ryan B, Wong Wylie DR (2007) Antigenic compartmentation of the hummingbird cerebellar cortex. Program No. 830.6.Abstract Viewer/Itinerary Planner. Washington, DC: Society for Neuroscience.

Ji Z, Hawkes R (1994) Topography of Purkinje cell compartments and mossy fiber terminal fields in lobules II and III of the rat cerebellar cortex: spinocerebellar and cuneocerebellar projections. Neuroscience 61:935–954.

Karavanova I, Vasudevan K, Cheng J, Buonanno A (2007) Novel regional and developmental NMDA receptor expression patterns uncovered in NR2C subunit-beta-galactosidase knock-in mice. Mol Cell Neurosci 34:468–480.

King JS, Madtes P Jr, Bishop GA, Overbeck TL (1997) The distribution of corticotropin-releasing factor (CRF), CRF binding sites and CRF_1 receptor mRNA in the mouse cerebellum. Prog Brain Res 114:55–66.

Lannoo MJ, Brochu G, Maler L, Hawkes R (1991) Zebrin II immunoreactivity in the rat and in the weakly electric teleost *Eigenmannia* (Gymnotiformes) reveals three modes of Purkinje cell development. J Comp Neurol 310:215–233.

Larouche M, Che P, Hawkes R (2006) Neurogranin expression identifies a novel array of Purkinje cell parasagittal stripes during mouse cerebellar development. J Comp Neurol 494:215–227.

Larouche M, Hawkes R (2006) From clusters to stripes: the developmental origins of adult cerebellar compartmentation. Cerebellum 5:77–88.

Linnarsson S, Mikaels A, Baudet C, Ernfors P (2001) Activation by GDNF of a transcriptional program repressing neurite growth in dorsal root ganglia. Proc Natl Acad Sci U S A 98:14681–14686.

Liu Q, Xie F, Siedlak SL, Nunomura A, Honda K, Moreira PI, Zhua X, Smith MA, Perry G (2004) Neurofilament proteins in neurodegenerative diseases. Cell Mol Life Sci 61:3057–3075.

Luckner R, Obst-Pernberg K, Hirano S, Suzuki ST, Redies C (2001) Granule cell raphes in the developing mouse cerebellum. Cell Tissue Res 303:159–172.

Marani E, Voogd J (1979) The morphology of the mouse cerebellum. Acta Morphol Neerl Scand 17:33–52.

Marzban H, Chung S, Watanabe M, Hawkes R (2007) Phospholipase Cβ4 expression reveals the continuity of cerebellar topography through development. J Comp Neurol 502:857–871.

McAndrew PE, Frostholm A, Evans JE, Zdilar D, Goldowitz D, Chiu IM, Burghes AH, Rotter A (1998) Novel receptor protein tyrosine phosphatase (RPTPrho) and acidic fibroblast growth factor (FGF-1) transcripts delineate a rostrocaudal boundary in the granular layer of the murine cerebellar cortex. J Comp Neurol 391:444–455.

Mugnaini E (1983) The length of cerebellar parallel fibers in chicken and rhesus monkey. J Comp Neurol 220:7–15.

Nakamura M, Sato K, Fukaya M, Araishi K, Aiba A, Kano M, Watanabe M (2004) Signaling complex formation of phospholipase Cβ4 with metabotropic glutamate receptor type 1alpha and 1,4,5-triphosphate receptor at the perisynapse and endoplasmic reticulum in the mouse brain. Eur J Neurosci 20:2929–2944.

Ozol K, Hawkes R (1997) The compartmentation of the granular layer of the cerebellum. Histol Histopathol 12:171–184.

Ozol K, Hayden JM, Oberdick J, Hawkes R (1999) Transverse zones in the vermis of the mouse cerebellum. J Comp Neurol 412: 95–111.

Pakan JMP, Iwaniuk AN, Wong Wylie DR, Hawkes R, Marzban H (2007) Purkinje cell compartmentation as revealed by zebrin II expression in the cerebellar cortex of pigeons (*Columba livia*). J Comp Neurol 501:619–630.

Paradies MA, Eisenman LM (1993) Evidence of early topographic organization in the embryonic olivocerebellar projection: a model system for the study of pattern formation processes in the central nervous system. Dev Dyn 197:125–145.

Pijpers A, Apps R, Pardoe J, Voogd J, Ruigrok TJ (2006) Precise spatial relationships between mossy fibers and climbing fibers in rat cerebellar cortical zones. J Neurosci 26:12067–12080.

Rogers JH, Ciossek T, Menzel P, Pasquale EB (1999) Eph receptors and ephrins demarcate cerebellar lobules before and during their formation. Mech Dev 87:119–128.

Sarna JR, Marzban H, Watanabe M, Hawkes R (2006) Complementary stripes of phospholipase Cβ3 and Cβ4 expression by Purkinje cell subsets in the mouse cerebellum. J Comp Neurol 496: 303–313.

Schilling K, Schmidt HH, Baader SL (1994) Nitric oxide synthase expression reveals compartments of cerebellar granule cells and suggests a role for mossy fibers in their development. Neuroscience 59:893–903.

Serafini T, Colamarino SA, Leonardo ED, Wang H, Beddington R, Skarnes WC, Tessier-Lavigne M (1996) Netrin-1 is required for commissural axon guidance in the developing vertebrate nervous system. Cell 87:1001–1014.

Sillitoe RV, Benson MA, Blake DJ, Hawkes R (2003) Abnormal dysbindin expression in cerebellar mossy fiber synapses in the mdx mouse model of Duchenne muscular dystrophy. J Neurosci 23:6576–6585.

Sillitoe RV, Hawkes R (2002) Whole-mount immunohistochemistry: a high-throughput screen for patterning defects in the mouse cerebellum. J Histochem Cytochem 50:235–244.

Sillitoe RV, Marzban H, Larouche M, Zahedi, Affanni J, Hawkes R (2005) Conservation of the architecture of the anterior lobe vermis of the cerebellum across mammalian species. Prog Brain Res 148:283–297.

Singec I, Knoth R, Ditter M, Frotscher M, Volk B (2003) Neurogranin expression by cerebellar neurons in rodents and non-human primates. J Comp Neurol 459:278–289.

Sotelo C, Chédotal A (2005) Development of the olivocerebellar system: migration and the formation of cerebellar maps. Prog Brain Res 148:1–20.

Sotelo C, Wassef M (1991) Cerebellar development: afferent organization and Purkinje cell heterogeneity. Phil Trans R Soc Lond B 331:307–313.

Sternberger LA, Sternberger NH (1983) Monoclonal antibodies distinguish phosphorylated and nonphosphorylated forms of neurofilaments in situ. Proc Natl Acad Sci U S A 80:6126–6130.

Sugihara I, Quy PN (2007) Identification of aldolase C compartments in the mouse cerebellar cortex by olivocerebellar labeling. J Comp Neurol 500:1076–1092.

Swanson DJ, Tong Y, Goldowitz D (2005) Disruption of cerebellar granule cell development in the Pax6 mutant, Sey mouse. Dev Brain Res 160:176–193.

Vastagh C, Vig J, Hámori J, Takács J (2005) Delayed postnatal settlement of cerebellar Purkinje cells in vermal lobules VI and VII of the mouse. Anat Embryol (Berl) 209:471–484.

Voogd J, Pardoe J, Ruigrok TJ, Apps R (2003) The distribution of climbing and mossy fiber collateral branches from the copula pyramidis and the paramedian lobule: congruence of climbing fiber cortical zones and the pattern of zebrin banding within the rat cerebellum. J Neurosci 23:4645–4656.

Voogd J, Ruigrok TJ (2004) The organization of the corticonuclear and olivocerebellar climbing fiber projections to the rat cerebellar vermis: the congruence of projection zones and the zebrin pattern. J Neurocytol 33:5–21.

Wassef M, Angaut P, Arsenio-Nunes L, Bourrat F, Sotelo C (1992a) Purkinje cell heterogeneity: its role in organizing the topography of

the cerebellar cortex connections. In: The cerebellum revisited (Llinás R, Sotelo C, eds), pp 5–21. New York: Springer.
Wassef M, Cholley B, Heizmann CW, Sotelo C (1992b) Development of the olivocerebellar projection in the rat: II. Matching of the developmental compartmentations of the cerebellum and inferior olive through the projection map. J Comp Neurol 323:537–550.
Wassef M, Zanetta JP, Brehier A, Sotelo C (1985) Transient biochemical compartmentalization of Purkinje cells during early cerebellar development. Dev Biol 111:129–137.
Yamasaki T, Kawaji K, Ono K, Bito H, Hirano T, Osumi N, Kengaku M (2001) Pax6 regulates granule cell polarization during parallel fiber formation in the developing cerebellum. Development 128:3133–3144.

(Accepted 13 February 2008)
(Available online 29 February 2008)